Appl Phys A (2011) 103:933–938
DOI 10.1007/s00339-011-6394-0

Applied Physics A
Materials Science & Processing

INVITED PAPER

Geometry-controlled adhesion: revisiting the contact splitting hypothesis

Michael Varenberg · Boris Murarash · Yuri Kligerman · Stanislav N. Gorb

Received: 28 March 2011 / Accepted: 6 April 2011 / Published online: 5 May 2011

Abstract Following studies of biological attachment systems, the principle of contact splitting, according to which splitting up the contact into finer subcontacts increases adhesion, was introduced. However, numerous attempts at employing this principle in producing dry adhesives were unsuccessful, prompting us to test its validity. Here, we show that in addition to the increase in number of subcontacts, the contact splitting model also implies a built-in increase in contact area. Thus, based on this model, it is impossible to say which parameter leads to increase in adhesion, the increasing number of subcontacts, as accepted to think, or just an increase in contact area, which is a trivial result. To clarify this point, we show experimentally what happens if we keep the contact area constant, while increasing the number of subcontacts in the "equal load sharing" mode, which was never done before. In contrast to the contact splitting principle, our measurements clearly demonstrate that, in flat-punch-patterned conformal contact, the pull-off force remains the same even when the number of subcontacts increases by two orders of magnitude. Our finding suggests that the contact splitting idea can only work in thin-film-based contacts, which are indeed employed in most biological temporary attachment systems.

M. Varenberg (✉) · B. Murarash · Y. Kligerman
Department of Mechanical Engineering, Technion-IIT, Haifa 32000, Israel
e-mail: michaelv@technion.ac.il

S.N. Gorb (✉)
Department of Functional Morphology and Biomechanics, Zoological Institute of the University of Kiel, Kiel 24098, Germany
e-mail: sgorb@zoologie.uni-kiel.de

1 Introduction

The ability of some animals to adhere to uneven surfaces while in motion has received much research attention during the last decade, resulting in a growing mass of literature (more than 250 published works to date). It is possible to sort these works into three groups: those describing complex biological systems, those trying to abstract the physical principles behind their impressive performance, and those attempting to build simpler artificial systems able to function in the same way. It is obvious that these groups belong to three different stages of research that ideally follow one another, so misinterpretation of earlier results may lead to incorrect conclusions at a later stage.

Following studies of hairy attachment pads evolved in different animal groups, an interesting correlation between the size of attachment hairs and animal weight was found: the heavier the animal, the smaller and more densely packed the hairs [1]. Based on this correlation and taking into account another set of observations showing that hairy attachment functions due to secretion-mediated capillary attraction forces and van der Waals interactions [2–5], the principle of contact splitting was introduced [6]. According to this principle, as it was understood in many subsequent works, splitting up the contact into finer subcontacts (of the same total contact area [7–9]) increases adhesion. However, numerous attempts at employing this principle in manufacturing dry adhesives were surprisingly unsuccessful. In most cases, simple arrays of micropillars [10–16] have not exhibited a stronger adhesion than flat controls made of the same materials, leading researchers to start experimenting with pillar terminals [16–22]. To this end, in light of the consistently observed discrepancy between theory and practice, we decided to test the validity of the principle of contact splitting.

2 Analysis of contact splitting model

The concept of contact splitting [6] was devised based on studying the adhesive behavior of contact elements characterized by self-similar scaling (radius of contact element is linearly related to its size) or curvature invariance (radius of contact element is independent of its size). For self-similar scaling, the areal density of contact elements, N, is expected to scale as $N = 4k^2m^{2/3}$, where k is a geometry-insensitive parameter and m is a mass to be supported by the adhesion force in the field of gravitation. For curvature invariance, the areal density of contact elements, N, is expected to scale as $N = kR^{-1}m^{1/3}$, where R is a contact element radius. It is clear that the latter case is preferable as it allows supporting the same mass with less contact elements of a larger radius.

By analyzing the preferred case of curvature invariance, we come to the following result. As a first step, the attachment pad is modeled by a single hemisphere, whose geometry is presented in Fig. 1a according to the JKR approach [23]. The contact area is small, compared to the apparent area of the attachment pad, and the pull-off force to be generated, F, is estimated by $F = 1.5\pi R\gamma$, where γ is the work of adhesion. To utilize the apparent area more efficiently, we take n segments of the above-mentioned hemisphere able to cover the apparent area of the attachment pad as shown in Fig. 1b. In this case, the contact area is n times the initial one and the pull-off force to be generated, F', is calculated by $F' = nF$. To utilize the apparent area even more, we will take p smaller segments of the same hemisphere and cover the attachment pad area as shown in Fig. 1c, making the contact area p times the initial one, which will result in a larger pull-off force $F'' = pF > nF$. Continuing in the same way, in the limit we will reach the ultimate result: maximum possible pull-off force will be achieved when the contact area approaches the apparent area of the attachment pad.

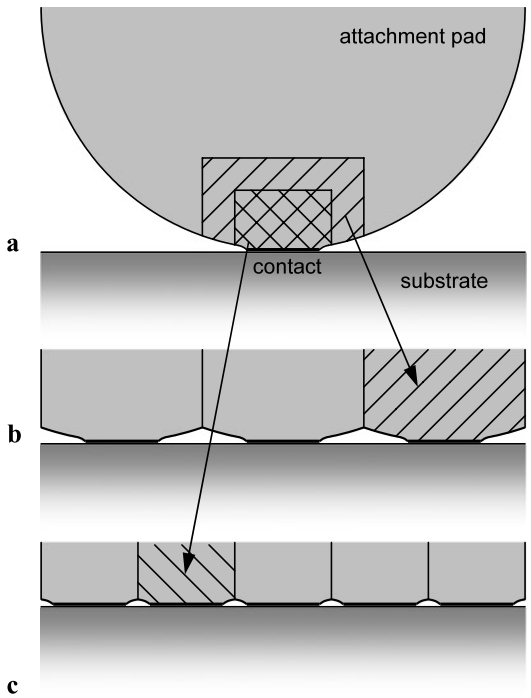

Fig. 1 Graphical representation of the contact splitting model. Real contact is indicated by the thick line

Thus, it appears that, according to this model, pull-off force grows with an increase in contact area, which is a trivial result. The question to be asked is whether splitting the contact can affect its adhesive performance if the total contact area remains unchanged. Considering the biological data, we can see two different ways of contact splitting that allow retaining the same contact area. The first is to split the contact into finer subcontacts based on flat protrusions similar to those found in bush crickets (Fig. 2a) [1] and tree frogs [24]. The second is to split the contact into finer subcontacts based on thin-film-ended surface elements similar

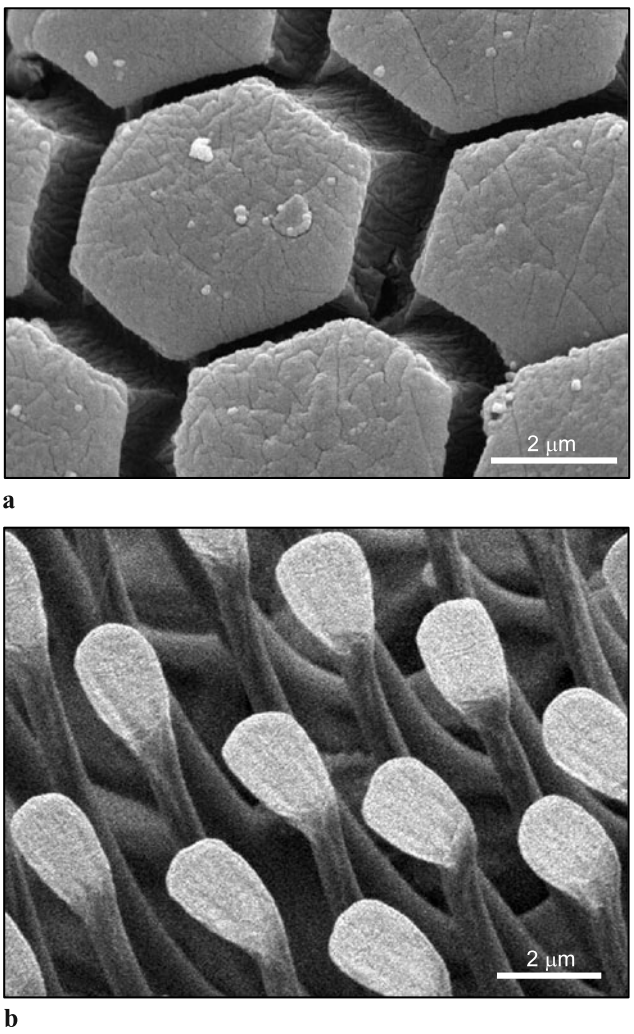

Fig. 2 Two different ways of biological contact splitting. (**a**) Flat protrusions evolved in attachment pad of great green bush cricket *Tettigonia viridissima*. (**b**) Thin-film-ended hairs evolved in attachment pad of the blue bottle fly *Calliphora vicina*

to those found in flies (Fig. 2b) [1], beetles [1, 2], geckos [1, 3], etc. To answer the above question, in the following we will discuss both types of contact splitting.

3 Elimination of contact area effect

3.1 Splitting into flat protrusions

3.1.1 Methods

The effect of contact splitting on pull-off force of flat protrusions was studied experimentally by testing 4 patterned poly(vinylsiloxane) (PVS, Coltène Whaledent AG, Altstätten, Switzerland) surfaces consisting of hexagonal contact plates of 10, 20, 50, or 95 µm in size and 1 µm in height, which were uniformly distributed all having the same contact area fraction of 75% (Fig. 3a). We tested plates of only one height as pull-off force measured in conformal contact is independent of the aspect (height over diameter) ratio of the pattern elements, as shown in additional set of tests (see below). To determine the influence of contact area, the tested surfaces were also compared with 4 other patterned PVS surfaces consisting of hexagonal dimples of the same sizes but having a contact area fraction of only 25% (Fig. 3b), as well as with a smooth PVS control having a contact area fraction of 100%.

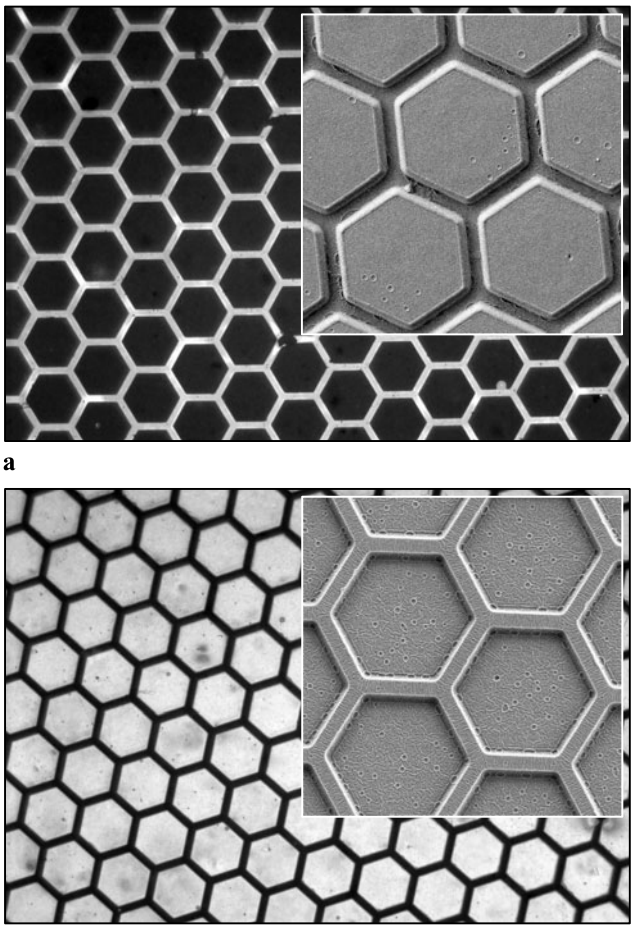

a

b

Fig. 3 Optical microscopy images of real contact between PVS and glass specimens. Destructive interference of a reflected white light results in a visualization of the real contact as a much darker zone than the area out of contact. (**a**) Hexagonal plates. (**b**) Hexagonal dimples. Inserts present SEM images of patterned surfaces. The *hexagons* presented are 20 µm in size (side length 10 µm)

Patterned surfaces were produced by pouring polymerizing PVS into the steel negative templates (OVD Kinegram, Zug, Switzerland). Smooth and patterned disks of 2 mm in diameter and 1 mm in height were punched out of the PVS cast. Ten individual specimens of each of the 9 types (1 smooth, 4 plate-patterned, and 4 dimple-patterned) were tested against a smooth glass substrate. The roughness average (R_a) of the PVS and glass surfaces was about 85 and 1 nm, respectively. The temperature and relative humidity in the laboratory were 23°C and 21%, respectively.

To prove that pull-off force measured in conformal contact is indeed independent of the pattern aspect ratio, we tested patterned poly(dimethylsiloxane) (PDMS, Sylgard 184, Dow Corning Co., Midland, Michigan) surfaces consisting of hexagonal contact plates of 50 µm in size and 10, 30, or 50 µm in height, which were distributed uniformly having the contact area fraction of 20, 40, 60, and 80%. Structured surface was produced by molding PDMS on the negative template prepared by photolithographic patterning of an SU-8 photoresist covering Si wafer. A 10:1 ratio of Sylgard 184 pre-polymer and cross-linker was cured for 14 h at 65°C in light vacuum to ensure complete filling of the template [15]. Samples of 2 mm in diameter were punched out of the 1 mm-height PDMS cast using disposable biopsy Uni-Punch (Premier Products Co., Plymouth Meeting, Pennsylvania). Ten individual specimens of each type were tested against a smooth glass substrate. The roughness averages (R_a) of the glass and PDMS surfaces were 5 and 50 nm, respectively. The temperature and relative humidity in the laboratory were 24°C and 52%, respectively.

Before use, the specimens were washed with deionized water and liquid soap, and dried in a flow of nitrogen gas. The tests were performed on home-made tribometers capable to determine pull-off force in a flat-on-flat contact scheme using a self-aligning system of sample holders [25] to fulfill the "equal load sharing" principle [12]. Each test began by bringing the polymer specimen in contact with the glass substrate and applying a normal load of either 60 mN in case of PVS or 100 mN in case of PDMS (as preload has no effect on pull-off force once the maximum possible contact area is reached [19], we tested only one load in each material). The pull-off force was measured while withdrawing the loading stage at a velocity of 100 μm/s. Prior to the next experiment, both the polymer and glass specimens were replaced with new ones.

3.1.2 Results

Figure 4 presents the pull-off force data obtained for smooth and micropatterned PVS surfaces detaching from a smooth glass substrate. The pull-off forces measured on plate-patterned surfaces of different characteristic sizes (Fig. 4a) display no statistically significant difference ($F = 2.153$, $P = 0.111$, One Way Analysis of Variance) even though the number of elements in contact increases by almost two orders of magnitude (from ~400 to ~36300). This observation allows suggesting that in practice, when stress concentrators and defects are always present at the contact edges, there is no slowdown in interface crack propagation due to just splitting the contact into smaller subcontacts, which was thought leading to adhesion enhancement earlier [12]. The dimple-patterned surfaces demonstrate the same result: as long as the contact area remains the same, there is no difference in pull-off force ($F = 0.445$, $P = 0.722$, One Way Analysis of Variance) no matter how the contact is split (Fig. 4a).

This behavior allows us to pool the data on different micropattern dimensions, showing a statistically significant difference between smooth, plate- and dimple-patterned surfaces ($H = 65.84$, $P < 0.001$, Kruskal-Wallis One Way Analysis of Variance on Ranks) and present pull-off force as a function of real contact area (Fig. 4b), demonstrating a clear correlation between the two parameters.

To prove that the above results reflect the behavior of higher pattern elements as well, we have also tested the effect of aspect ratio on pull-off force of plate-patterned PDMS surfaces, as shown in Fig. 5. Based on these data, the lack of correlation between the pull-off force measured in conformal contact and the aspect ratio of the patterned surface becomes evident. Analyzing this data set statistically, we obtain the same result: there is no significant difference in pull-off forces measured on the patterned surfaces of different aspect ratios ($H = 0.942$, $P = 0.624$, Kruskal–Wallis One Way Analysis of Variance on Ranks, data on different contact area fraction are pooled together).

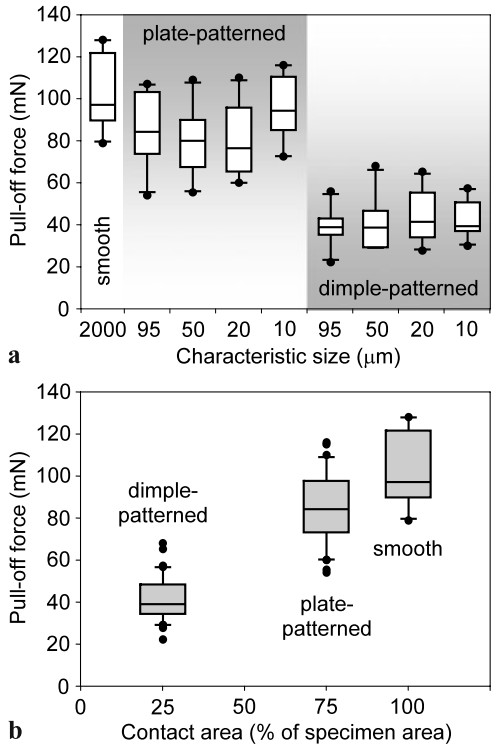

Fig. 4 Pull-off force of smooth and patterned PVS surfaces measured against glass flat. (**a**) Complete data set. (**b**) The data on different micropattern sizes are pooled together and shown as a function of contact area. The data is presented using box-and-whisker diagrams, where the bottom and top of the box are the 25th and 75th percentiles, the band inside the box is the median, the ends of the whiskers are the 10th and 90th percentiles, and the dots are outliers

3.1.3 Discussion

It is worth mentioning that the above finding contradicts our own previous report on the absence of effect of real contact area that suggested that the real contact perimeter is the main geometrical factor governing adhesion [26]. However, in view of the recent works showing a significant influence of the shape of terminal contact elements [16, 18–20], the fact that the surface structures tested in the discussed work [26] consisted of pillars with different terminal elements (mushroom-shaped and flat-punch-ended) discredits this earlier suggestion.

Interestingly, there is evidence that in some cases artificial flat-punch-ended fibrillar adhesives perform better than flat surfaces made of the same materials [15, 16, 27], which requires an explanation. The pull-off force, F, is defined by the difference between the adhesion force, A, arising due to van der Waals or capillary interaction and contact reaction

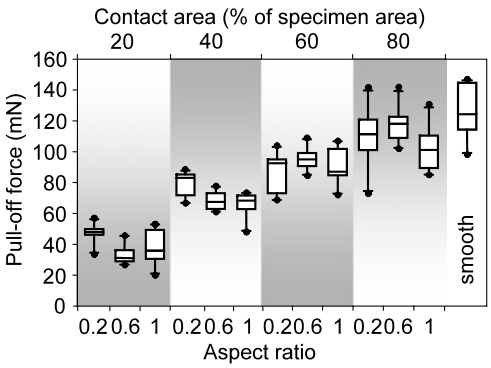

Fig. 5 Pull-off force of plate-patterned PDMS surfaces as a function of aspect ratio of the pattern elements distributed with different contact area fraction. The data is presented using box-and-whisker diagrams, where the bottom and top of the box are the 25th and 75th percentiles, the band inside the box is the median, the ends of the whiskers are the 10th and 90th percentiles, and the dots are outliers

force, C, arising due to storage of elastic energy during contact deformation, $F = A - C$. In light of the above, it is clear that splitting the contact pad based on flat protrusions is unable to affect adhesion, $A_{\text{full}} = A_{\text{split}} = A$. However, it may significantly decrease the contact stiffness, S, thus affecting reaction force, $C = f(S)$, when in nonconformal contact, such as in a widely used sphere-on-flat contact test scheme. In contrast to conformal contact, where regardless of the contact stiffness fibrillar elements always share the same load, so $F = A - C \cong A$ as $C \to 0$ at the very moment of maximum resistance to pulling-off, in a sphere-on-flat contact the picture is different: some fibrillar elements may remain in a compressed state even at the very moment of maximum resistance to pulling-off, so $F = A - C < A$ as $C \neq 0$. Hence, the measured pull-off force, F, increases with decreasing the contact stiffness, S, which changes as a function of the length over diameter ratio of contact elements. In this case, the structured surfaces consisting of finer contact elements demonstrate higher pull-off force [15, 16], giving the impression that the principle of contact splitting [6] allows increasing adhesion when retaining the same contact area. Comparing the adhesive performance of structured surfaces with that of flat reference may lead to further confusion. The flat reference has larger contact area resulting in higher adhesion, $A_{\text{ref}} > A_{\text{split}}$, and larger contact stiffness resulting in higher reaction force, $C_{\text{ref}} > C_{\text{split}}$, so its measured pull-off force, $F_{\text{ref}} = A_{\text{ref}} - C_{\text{ref}}$, may be either higher or lower than that of structured contact, $F_{\text{split}} = A_{\text{split}} - C_{\text{split}}$, which increases when using finer contact elements.

Use of much stiffer materials for mimicking dry biological adhesives [27] leads to the same interrelation between adhesion and reaction forces. Real contact area formed under a given load depends on contact stiffness even in a conformal contact, and as larger contact area is achieved when using a split contact, the latter features higher adhesion and pull-off force.

Another point that should be mentioned with regard to contact splitting based on flat protrusions is that in light of the above results it becomes clear that the surface micropattern evolved in attachment pads of bush crickets [1] and tree frogs [24] is not used for adhesion enhancement. This and similar surface micropatterns evolved in smooth attachment pads [1] of different animals are used mainly to control frictional properties of contact by eliminating stick-slip and hydroplaning effects, as was clearly demonstrated in our previous study [28].

3.2 Splitting into thin-film elements

3.2.1 Discussion

The effect of contact splitting on adhesion of thin-film-ended surface elements of constant contact area was recently

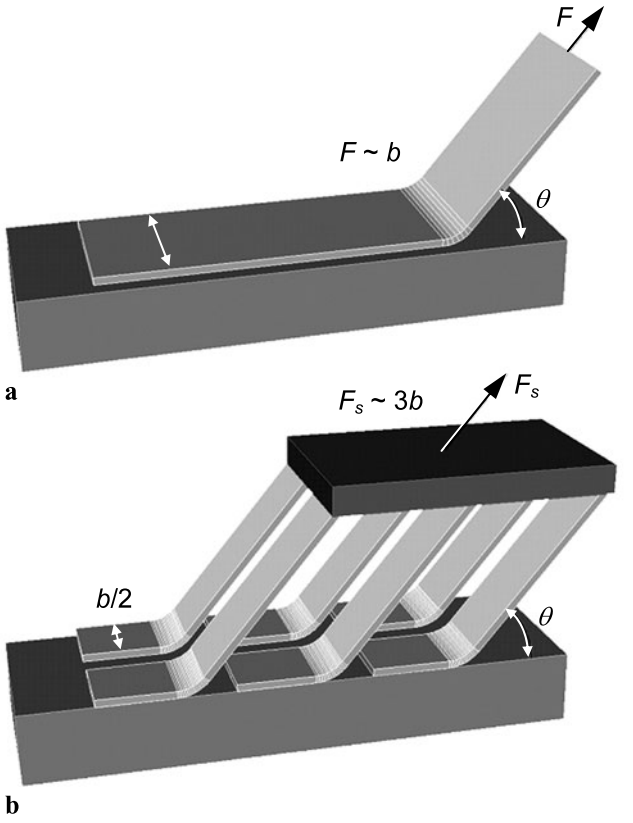

Fig. 6 Graphical representation of the effect of adhesion enhancement by increasing the peeling line length [29]. (**a**) A single piece of elastic film peeling from a rigid substrate. Peeling force F is proportional to the film width b (at constant peel angle θ for given pair of materials). (**b**) A series of elastic films covering the same contact area as in (**a**). Peeling force F_s is threefold the value F in (**a**) due to an overall growth of the peeling line length calculated as a sum of individual film widths

analyzed [29] using the Kendall peeling model [30]. The analysis made had shown that an attachment ability of a split contact grows (regardless of the contact area) with an overall length of the peeling line, which is the sum of widths of all thin-film elements participating in contact (Fig. 6). This approach allows to show that tenfold-smaller thin-film elements, packed with the same areal density on the same area, give a tenfold-larger overall peeling line and, hence, peeling force, which explains the scaling effects observed in biological fibrillar attachment systems [1].

Despite much research activity, thin-film-based fibrillar biomimetic surface structures have not been fabricated so far due to various technological limitations, so direct experimental proof of the peeling line idea is not yet possible. However, applying the peeling line approach to biological fibrillar attachment devices, we found that the total peeling line achievable in attachment pads of such animals as flies, beetles, mites, spiders, anoles and geckos is closely correlated with their body mass [29]. This latter finding allows us to suggest that splitting up the contact into finer subcontacts

based on thin-film-ended surface elements is indeed the way leading to adhesion enhancement.

4 Conclusion

Based on the study performed, it appears that splitting up the contact based on flat protrusions may only enhance its adaptivity [15, 16, 27] or resistance to contamination [19, 31] but has no effect on its adhesive properties if contact area does not change. This finding provides an explanation of why biological fibrillar adhesive systems almost never rely on flat-punch or hemisphere-ended structures. The study suggests that to construct a successful dry adhesive, it is necessary to implement thin-film-based terminal elements at the tip of each contact protuberance.

Acknowledgement We thank Achim Hansen and Andreas Schilling for providing micropattern templates. This work, as part of the German Science Foundation (DFG) Initiative "Bionik," was supported by the DFG grant GO995/7-1 to S.G.

References

1. M. Scherge, S.N. Gorb, *Biological Micro- and Nanotribology: Nature's Solutions* (Springer, Berlin, 2001)
2. N.E. Stork, J. Exp. Biol. **88**, 91 (1980)
3. K. Autumn, Y.A. Liang, S.T. Hsieh, W. Zesch, W.P. Chan, T.W. Kenny, R. Fearing, R.J. Full, Nature **405**, 681 (2000)
4. K. Autumn, M. Sitti, Y.A. Liang, A.M. Peattie, W.R. Hansen, S. Sponberg, T.W. Kenny, R. Fearing, J.N. Israelachvili, R.J. Full, Proc. Natl. Acad. Sci. USA **99**, 12252 (2002)
5. G. Huber, H. Mantz, R. Spolenak, K. Mecke, K. Jacobs, S.N. Gorb, E. Arzt, Proc. Natl. Acad. Sci. USA **102**, 16293 (2005)
6. E. Arzt, S. Gorb, R. Spolenak, Proc. Natl. Acad. Sci. USA **100**, 10603 (2003)
7. E. Arzt, Mater. Sci. Eng., C, Biomim. Mater., Sens. Syst. **26**, 1245 (2006)
8. E.P. Chan, C. Greiner, E. Arzt, A.J. Crosby, Mater. Res. Soc. Bull. **32**, 496 (2007)
9. E. Kroner, E. Arzt, Vak. Forsch. Prax. **21**, A14 (2009)
10. M. Sitti, R.S. Fearing, J. Adhes. Sci. Technol. **17**, 1055 (2003)
11. N.J. Glassmaker, A. Jagota, C.-Y. Hui, J. Kim, J. R. Soc. Interface **1**, 23 (2004)
12. C.-Y. Hui, N.J. Glassmaker, T. Tang, A. Jagota, J. R. Soc. Interface **1**, 35 (2004)
13. A. Peressadko, S.N. Gorb, J. Adhes. **80**, 247 (2004)
14. B. Aksak, M.P. Murphy, M. Sitti, Langmuir **23**, 3322 (2007)
15. C. Greiner, A. del Campo, E. Arzt, Langmuir **23**, 3495 (2007)
16. A. del Campo, C. Greiner, E. Arzt, Langmuir **23**, 10235 (2007)
17. S. Kim, M. Sitti, Appl. Phys. Lett. **89**, 261911 (2006)
18. N.J. Glassmaker, A. Jagota, C.-Y. Hui, W.L. Noderer, M.K. Chaudhury, Proc. Natl. Acad. Sci. USA **104**, 10786 (2007)
19. S. Gorb, M. Varenberg, A. Peressadko, J. Tuma, J. R. Soc. Interface **4**, 271 (2007)
20. L. Qu, L. Dai, M. Stone, Z. Xia, Z.L. Wang, Science **322**, 238 (2008)
21. M.P. Murphy, B. Aksak, M. Sitti, Small **5**, 170 (2009)
22. C. Greiner, E. Arzt, A. del Campo, Adv. Mater. **21**, 479 (2009)
23. K.L. Johnson, K. Kendall, A.D. Roberts, Proc. R. Soc. Lond. Ser. A, Math. Phys. Sci. **324**, 301 (1971)
24. W.J.P. Barnes, Mater. Res. Soc. Bull. **32**, 479 (2007)
25. M. Varenberg, A. Peressadko, S. Gorb, E. Arzt, S. Mrotzek, Rev. Sci. Instrum. **77**, 066105 (2006)
26. M. Varenberg, A. Peressadko, S. Gorb, E. Arzt, Appl. Phys. Lett. **89**, 121905 (2006)
27. A.K. Geim, S.V. Dubonos, I.V. Grigorieva, K.S. Novoselov, A.A. Zhukov, Nat. Mater. **2**, 461 (2003)
28. M. Varenberg, S. Gorb, Adv. Mater. **21**, 483 (2009)
29. M. Varenberg, N.M. Pugno, S.N. Gorb, Soft Matter **6**, 3269 (2010)
30. K. Kendall, J. Phys. D, Appl. Phys. **8**, 1449 (1975)
31. W.R. Hansen, K. Autumn, Proc. Natl. Acad. Sci. USA **102**, 385 (2005)